

in 65 nm CMOS process, In: IEEE Asia Pacific Microwave Conference, Singapore, 2009, pp. 2268–2271.

7. M.-C. Chen and C.-Y. Wu, Design and analysis of CMOS subharmonic injection-locked frequency triplers, IEEE Trans Microwave Theory Tech 56 (2008), 1869–1878.
8. C.-Y. Wu, M.-C. Chen, and Y.-K. Lo, A phase-locked loop with injection-locked frequency multiplier in 0.18- μm CMOS for V-band applications, IEEE Trans Microwave Theory Tech 57 (2009), 1629–1636.

© 2012 Wiley Periodicals, Inc.

A DUAL-MODULUS INJECTION-LOCKED FREQUENCY DIVIDER WITH LARGE LOCKING RANGE

Wei Zhang,¹ Liang Zhang,¹ Xu Zhang,¹ and Yanyan Liu²

¹ School of Electronic Information Engineering, Tianjin University, Tianjin 300072, China

² College of Information Technical Science, Nankai University, Tianjin 300071, China; Corresponding author: lytianjin@nankai.edu.cn

Received 13 May 2012

ABSTRACT: A dual-modulus of 2/3 injection-locked frequency divider with wide locking ranges is presented in this work. It uses an active inductor as the resonance loop, and a tunable active-resistance is introduced to control the operation point and reinforce the injection efficiency. Simulations and measurements show that the proposed design can realize large locking ranges without any extra tuning, and cost low power consumption and small area. The divider was fabricated under the Chartered 0.35 μm CMOS technology, and the chip area is about 544 μm^2 . Measurements show that it has locking ranges from 1.5 to 2.05 GHz and 1.74 to 1.95 GHz at 0 dBm input power for divide-by-2 and -3, respectively, and the power consumed is only about 1.49 mW. © 2012 Wiley Periodicals, Inc. Microwave Opt Technol Lett 55:269–272, 2012; View this article online at wileyonlinelibrary.com. DOI 10.1002/mop.27290

Key words: injection-locked frequency divider; dual-modulus division; large locking range; tunable active-resistance; tunable active inductance

1. INTRODUCTION

In recent years, lots of demand for the high-speed data transferring with the compact implementation have stimulated communication systems to increase their working speed and enlarge the bandwidth [1, 2]. In high-speed communication systems, such as phase-locked loops, high-speed frequency dividers play a critical role in determining the final performance [3–5].

Commonly used dividers are based on the current mode logic structure. When the frequency increases, they cost more power, and the highest operating frequency is limited. As an alternative, injection-locked frequency dividers (ILFDs) have lower power dissipation and higher operating speed. However, it is relatively hard for ILFDs to realize multimodulus division.

To solve above problem, ring oscillators are adopted, because they are tunable by changing the number of cascades. LC/RC differential oscillators are also used for multi even or odd ratios. However, intrinsic characteristics of above types, such as low speed of ring oscillators and difficulty of integration for LC ones, limit their applications [6]. In addition, most works mainly focus on multimodulus divisions, the ILFDs can only work under discrete frequency bands for different ratios, and their locking range is often narrow.

In this article, a direct inject ILFD based on a differential active inductance oscillator is proposed. By switching an active

tunable resistance (TAR) fixed at the common source of differential pairs, the operation point of the active inductor is changed, and division ratios of 2 and 3 can be realized for a single frequency region. The locking range of divide-by-3 is also extended by harmonic reinforcement of the TAR.

2. THEORETICAL ANALYSIS

The basic ILFD based on the cross-coupled LC resonator is shown in Figure 1(a). To obtain more specific instructions, a mathematic model for above structure is illustrated in Figure 1(b).

The model indicates that after filtering and conversion of the core circuit, there is a mixing behavior between input and output signals, which help to realize frequency dividing. M is division ratio that is an integer and larger than 1. A represents the nonlinearity of the core circuit, and it can be approximated as,

$$A(x) = a_0 + a_1x + a_2x^2 + \dots \quad (1)$$

Then,

$$u = p + A(f_{\text{out}}) = B(f_{\text{in}} \times A(f_{\text{out}})) + A(f_{\text{out}}) \\ (2)(2) = B(f_{\text{in}} \times A(f_{\text{out}})) + a_0 + a_1(f_{\text{out}}) + a_2(f_{\text{out}})^2 + \dots \quad (2)$$

where B is the conversion gain. Substitute all parameters in Eq. (2), and we have,

$$u = B\{F_i \cos(M\omega_0 t) \times \\ [a_0 + a_1 F_o \cos(\omega_0 t + \theta_0) + a_2 (F_o \cos(\omega_0 t + \theta_0))^2 + \dots] \} \\ + [a_0 + a_1 F_o \cos(\omega_0 t + \theta_0) + a_2 (F_o \cos(\omega_0 t + \theta_0))^2 + \dots] \quad (3)$$

In Eq. (3), the first item on the right-hand side is the mixing component, and only the component of ω_0 from the product is effective. That is, in the first square bracket, the components of $(M - 1)$, $(M + 1)$, $(M + 3)$, and so on should be taken into account. As coefficients of higher terms are small, terms larger than $(M + 3)$ are ignored. Similarly, only the fundamental component and the third harmonic of the second item on the right-hand side are considered, which stands for the contribution of the output itself to the oscillation. Rearrange Eq. (3) as the follows,

$$u_{\text{eff}} = B\{F_i \cos(M\omega_0 t) \times [a_{M-1} (F_o \cos(\omega_0 t + \theta_0))^{M-1} \\ + a_{M+1} (F_o \cos(\omega_0 t + \theta_0))^{M+1}] \} \\ + [a_1 F_o \cos(\omega_0 t + \theta_0) + a_3 (F_o \cos(\omega_0 t + \theta_0))^3] \quad (4)$$

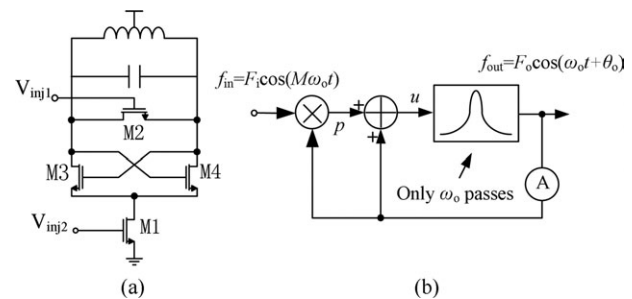


Figure 1 (a) Conventional structure of ILFD based on cross-coupled LC resonator. (b) An ILFD model

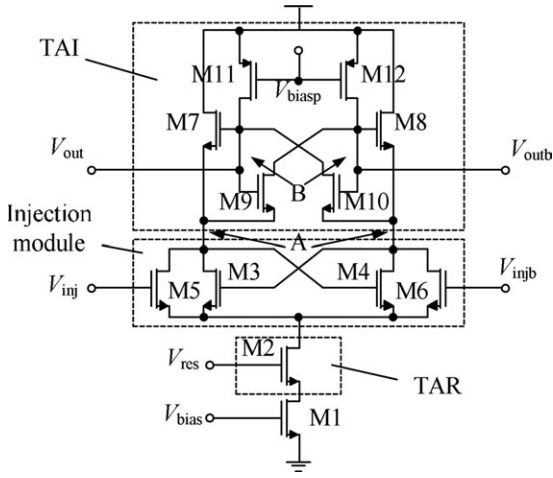


Figure 2 The proposed ILFD

where u_{eff} is composite signal only with effective components. We get the final result as Eq. (5),

$$\begin{aligned}
 u_{\text{eff}} = & B \left\{ \frac{a_{M-1} F_1 F_o^{M-1}}{2^{M-1}} \cos[\omega_o t - (M-1)\theta_o] + \right. \\
 & \frac{a_{M+1} F_i F_o^{M+1}}{2^M} \cos[\omega_o t - (M-1)\theta_o] + \\
 & \left. \frac{a_{M+1} F_i F_o^{M+1}}{2^{M+1}} \cos[\omega_o t + (M+1)\theta_o] \right\} \\
 & + \left[a_1 F_o \cos(\omega_o t + \theta_o) + \frac{1}{4} a_3 F_o^3 \cos(\omega_o t + \theta_o) \right] \\
 = & P_1 \cos[\omega_o t - (M-1)\theta_o] + P_2 \cos[\omega_o t + (M+1)\theta_o] \\
 & + P_3 \cos(\omega_o t + \theta_o)
 \end{aligned} \quad (5)$$

where

$$\begin{aligned}
 P_1 = & \frac{B \cdot a_{M-1} F_1 F_o^{M-1}}{2^{M-1}} + \frac{B \cdot a_{M+1} F_i F_o^{M+1}}{2^M} \\
 P_2 = & \frac{B \cdot a_{M+1} F_i F_o^{M+1}}{2^{M+1}} \\
 P_3 = & a_1 F_o + \frac{1}{4} a_3 F_o^3
 \end{aligned}$$

According to Barkhausen phase criterion and LCR tank's impedance formula, the loop phase shifting can be expressed as (6).

$$\angle u_{\text{eff}} + \tan^{-1} \left(\frac{R}{\omega L} \cdot \frac{\omega_r^2 - \omega^2}{\omega_r^2} \right) = \theta_o \quad (6)$$

where ω_r is the resonant frequency of LCR tank, and

$$\begin{aligned}
 \tan(\angle u_{\text{eff}}) = & \frac{-P_1 \sin[(M-1)\theta_o] + P_2 \sin[(M+1)\theta_o] + P_3 \sin(\theta_o)}{P_1 \cos[(M-1)\theta_o] + P_2 \cos[(M+1)\theta_o] + P_3 \cos(\theta_o)} \\
 \frac{R}{\omega L} \cdot \frac{\omega_r^2 - \omega^2}{\omega_r^2} = & \tan(\theta_o = \angle u_{\text{eff}}) \\
 = & \frac{\sin(\theta_o) \cos(\angle u_{\text{eff}}) - \cos(\theta_o) \sin(\angle u_{\text{eff}})}{\cos(\theta_o) \cos(\angle u_{\text{eff}}) + \sin(\theta_o) \sin(\angle u_{\text{eff}})} \\
 = & \frac{\sin(\theta_o) - \cos(\theta_o) \tan(\angle u_{\text{eff}})}{\cos(\theta_o) + \sin(\theta_o) \tan(\angle u_{\text{eff}})}
 \end{aligned} \quad (7)$$

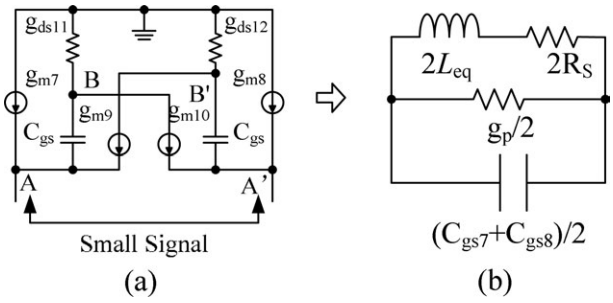


Figure 3 (a) Small signal model of TAI. (b) Equivalent RLC tank of TAI

Simplify Eq. (7), we get,

$$\frac{2\omega_L R}{\omega L \omega_r} = \left| \frac{P_1 \sin(M\theta_o) - P_2 \sin(M\theta_o)}{P_1 \cos(M\theta_o) + P_2 \cos(M\theta_o) + P_3} \right| \quad (8)$$

Considering the small injection condition, $P_1, P_2 \ll P_3$, we can use $M\theta_o = \frac{\pi}{2}$ to determine the locking range, ω_L , as

$$\frac{2\omega_L R}{\omega L \omega_r} \cong \left| \frac{P_1 - P_2}{P_3} \right| \quad (9)$$

$$\begin{aligned}
 \omega_L = & \left| \frac{P_1 - P_2}{P_3} \right| \cdot \frac{\omega_r}{2Q} \\
 = & \frac{B \cdot F_i \cdot (4a_{M-1} F_o^{M-1} + a_{M+1} F_o^{M+1})}{2^{M+1} (a_1 + \frac{1}{4} a_3 F_o^2)} \cdot \frac{\omega_r}{2Q} \\
 = & \eta \cdot \frac{\omega_r}{2Q}
 \end{aligned} \quad (10)$$

It should be noted that injection efficiency η is proportional to mixing harmonics' coefficients, a_{M-1}, a_{M+1} , and the convention gain. For divide-by-2, the fundamental and the third harmonic contribute more to the injection efficiency. That is, the wide locking range is anticipated by reinforcing these two frequency components. In the same way, the locking range of divide-by-3 can be extended by reinforcing the second and fourth harmonics.

3. CIRCUIT DESIGN

In Figure 1, transistors M1 and M2 can be chosen as injection points. However, such structure is adverse to the realization of divide-by-3 with the wide locking range [6]. Our design shown in Figure 2 solves the problem.

3.1. Tunable Active Inductance

According to Eq. (10), the quality factor should be lowered to widen the locking range. For this reason, a tunable active inductance (TAI) is introduced in the proposed ILFD. The small

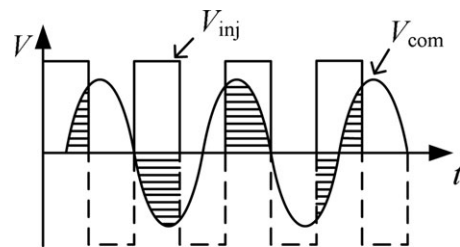


Figure 4 Operation of injection MOSFETs

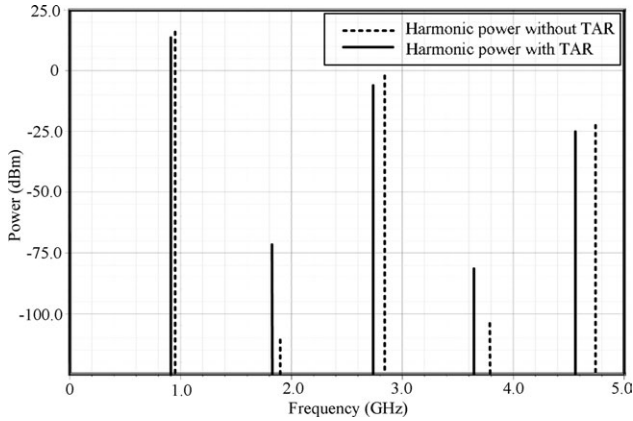


Figure 5 Simulation results of harmonic reinforcement

signal model of the TAI is shown in Figure 3(a). Figure 3(b) is its RLC counterpart.

$$L_{eq} = \frac{C_{gs}}{g_{ds11}(2g_{m9} - g_{ds11} + g_{m7})} \quad (11)$$

$$R_S = \frac{-g_{m5} + g_{ds11}}{g_{ds11}(2g_{m5} - g_{ds11} + g_{m3})} \quad (12)$$

$$g_p = g_{ds1} \quad (13)$$

$$C_{gs} = C_{gs7/8} || C_{gs9/10} \quad (14)$$

where C_{gs} is capacitance between the gate and the source region of a MOSFET, g_m is the transconductance, and g_{ds} is the conductance between the drain and the source region.

As shown in Eqs. (11) and (12), the equivalent inductance and resistance of the TAI are determined by the transconductances of MOSFETs. Therefore, a suitable quality factor can be obtained by choosing reasonable transconductances to realize the wide locking range.

3.2. Harmonic Reinforcement of Divide-by-3

As analyzed in Section 2, the second harmonic should be reinforced to extend the locking range of divide-by-3. Injection transistors can be treated as switches. Their working status is

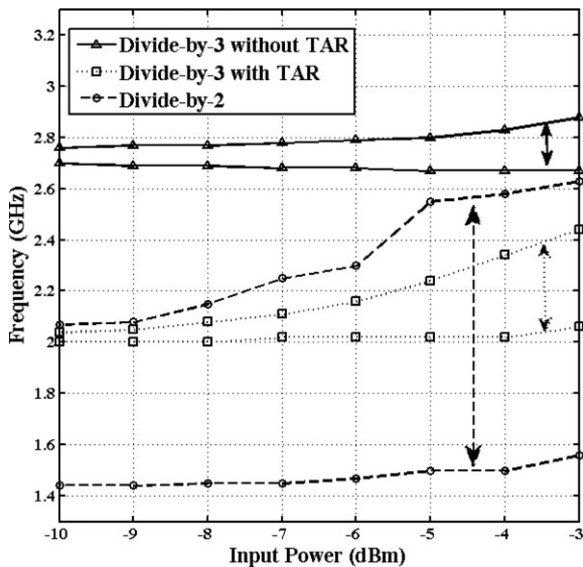


Figure 6 Simulation results of locking ranges

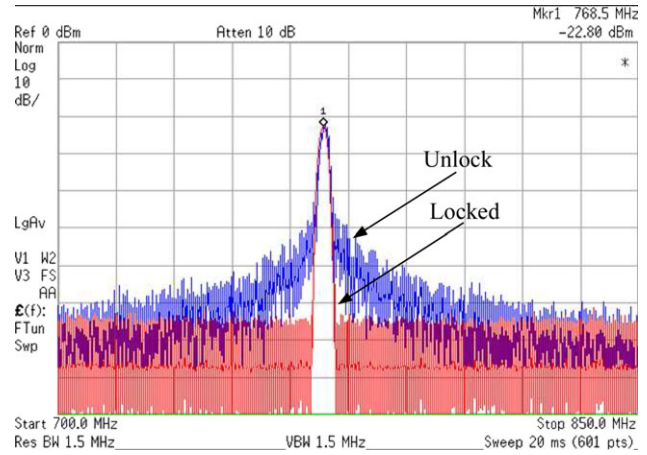


Figure 7 Spectrum measurement of the free-running mode and divide-by-2 with the input frequency of 1.537 GHz. [Color figure can be viewed in the online issue, which is available at wileyonlinelibrary.com]

shown in Figure 4. Where V_{com} represents the common mode signal in the common source point, and its frequency is twice as large as that of the fundamental.

Input signal has three times the frequency of the fundamental. The injection transistors conduct only in the overlapped shadow. According to saturation formula, the mixing product is,

$$\text{product} = \frac{\beta}{2} \cdot \{V_i - V_{co} \sin(2\omega_o + \sigma)\}^2 \cdot \left[\frac{1}{2} + \text{square}(3\omega_o) \right]^2 \quad (15)$$

where σ is the initial phase shifting. V_i and V_{co} are the amplitudes of the input and common mode signal, respectively.

A simple expression for the amplitude of ω_o component is given as,

$$A_{prod\omega_o} = \frac{V_{co}}{2\pi} [V_{co}^2 + 16V_i^2 - 8V_i V_{co} \sin(3\sigma)] \quad (16)$$

The product will increase with the enlargement of the even harmonics of the common mode to a certain extent no matter what σ is. Thus, the locking range of divide-by-3 is increased.

The tunable active resistance (TAR) as shown in Figure 2 is used to switch the division ratio, control the frequency, and enhance the even harmonics for the divide-by-3 mode. When the control signal V_{res} is "off" (the detailed value is determined

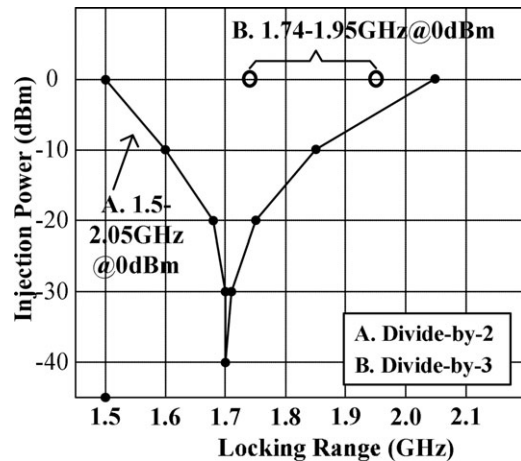


Figure 8 Measurement of locking range

TABLE 1 Performance Comparison of Two-Modulus ILFDs

Ref.	Processing (μm)	P_{in} (dBm)	VDD (V)	P_{diss} (mW)	Locking Range (± 2) (GHz)	Locking Range (± 3) (GHz)	Division Ratio	Tuning Varactor	Area (mm^2)
[3]	0.35	10	1.5	15.15	4.56–5.59 (20%)	6.9–8.4 (19%)	2 or 3	Y	0.6
[6]	0.18	5	1.8	12.51	3.18–4.05 (24%)	4.85–5.7 (16%)	2 or 3	Y	0.64
[7]	0.18	−0.5	1.8	3.15	3.44–5.02 (37%)	4.28–4.81 (11%)	2 or 3	Y	0.876
[8]	0.18	0	1.5	4.17	8.42–10.74 (24%)	13.66–14.96 (9%)	2 or 3	Y	0.35
This work	0.35	0	3.3	1.49	1.5–2.05 (31%)	1.74–1.95 (11%)	2 or 3	N	0.56

according to the results of simulations), the TAR is brought in to enhance the even harmonics. It should be noted that, because of existence of the TAR, the free running frequency of the divider can be adjusted with the variation of the bias current. The TAR and the TAI are combined to operate as a frequency controller, and the proposed ILFD can work in a single frequency band for different division ratios.

4. SIMULATION AND MEASUREMENT RESULTS

Simulations of the harmonic energy in the common mode point are carried out. The results are plotted in Figure 5. It shows that the power of the even harmonics is enlarged after the TAR is brought into the circuit. It can help to increase the product of injection mixing and then enlarge the locking range of the divide-by-3 mode. The locking ranges of proposed ILFD are shown in Figure 6.

The design was fabricated under Chartered 0.35 μm CMOS technology. The chip area is 0.56 mm^2 (544 μm^2 for core circuits), and the power consumption of the proposed ILFD is 1.49 mW. Spectrum measurements of the chip were carried out by Agilent E4443A PSA Spectrum Analyzer. The outputs of the free-running mode and divide-by-2 with 1.537 GHz input signal are shown in Figure 7.

The measured locking range versus input sensitivity is shown in Figure 8. Due to process variations and parasitic effects on the test board, the central frequency shown in Figure 8 shifts compared with simulation results. The locking range of divide-by-2 at input power of 0 dBm is from 1.5 to 2.05 GHz. The dividing function even can be achieved at a lowest input power of −40 dBm as shown in curve A. Curve B shows the divide-by-3 operation with the TAR, a locking range from 1.74 to 1.95 GHz is achieved. Compared with none TAR structure, which works from 2.88 to 2.98 GHz, the TAR circuit helps to adjust the free-running frequency, realize the dual-modulus division for a single band, and enlarge the locking range of the divide-by-3 mode.

Table 1 shows the comparison results of the proposed ILFD with some previous reports. It can be seen that although the frequency of our work is low due to the fabrication process with large feature size, the proposed divider still exhibits a wide locking range in both divide-by-2 and -3 modes without tuning varactor. In addition, with the only two statuses (on and off) for the TAR controlling, the divider can change its free-running frequency automatically, and the input signal can be in the same frequency region for both 2 and 3 division ratios. It means easy control and applications for multioutput frequencies in a single band.

5. CONCLUSION

In this article, the model for ILFD has been newly explored, and instructions for locking range enlargement were obtained. A two-modulus of 2/3 ILFD was designed and fabricated under Chartered 0.35 μm CMOS technology. Both the TAR and the TAI were used to enlarge the locking range. The ILFD exhibits wide locking ranges that can reach 31% for divide-by-2 and 11.4% for divide-by-3. Single band operation is also realized. The proposed divider

has a great advantage for the design of the first stage of low-power radio frequency front-ends with variable output frequencies.

ACKNOWLEDGMENT

This project is supported by the National Natural Science Foundation of China (Grant No. 61204028) and the Fundamental Research Funds for the Central Universities.

REFERENCES

1. B.-Y. Lin and S.-I. Liu, Analysis and design of D-band injection-locked frequency dividers, *IEEE J Solid-State Circuits* 46 (2011), 1250–1264.
2. Y.-T. Chen, M.-W. Li, H.-C. Kuo, T.-H. Huang, and H.-R. Chuang, Low-voltage K-band divide-by-3 injection-locked frequency divider with floating-source differential injector, *IEEE Trans Microwave Theory Tech* 60 (2012), 60–67.
3. S.-L. Jang, C.-Y. Lin, and C.-F. Lee, A low voltage 0.35 μm CMOS frequency divider with the body injection technique, *IEEE Microwave Wireless Compon Lett* 18 (2008), 470–472.
4. S.-L. Jang, C.-W. Tai, and C.-F. Lee, Divide-by-3 injection-locked frequency divider implemented with active inductor, *IEEE Microwave Wireless Compon Lett* 50 (2008), 1682–1685.
5. S.-L. Jang, J.-C. Han, C.-F. Lee, and J.-F. Huang, A small die area and wide locking range CMOS frequency divider, *Microwave Opt Technol Lett* 50 (2008), 541–544.
6. S.-L. Jang, C.-F. Lee, and W.-H. Yeh, A divide-by-3 injection locked frequency divider with single-ended input, *IEEE Microwave Wireless Compon Lett* 18 (2008), 142–144.
7. Y.-N. Miao, C.-C. Boon, M.-A. Do, K.-S. Yeo, and Y.-X. Zhang, High-frequency low-power LC divide-by-2/3 injection-locked frequency divider, *Microwave Opt Technol Lett* 53 (2011), 337–340.
8. S. Lyang, R.-K. Yang, C.-W. Chang, and M.-H. Juang, Multi-modulus LC injection-locked frequency dividers using single-ended injection, *IEEE Microwave Wireless Compon Lett* 19 (2009), 311–313.

© 2012 Wiley Periodicals, Inc.

COMPACT SINGLE-FEED CIRCULAR SLOT ANTENNA WITH ASYMMETRICAL C-SHAPED STRIPS FOR WLAN/WiMAX TRIBAND AND CIRCULAR/ELLIPTICAL POLARIZATIONS

Chia-Yen Wei,¹ Ji-Chyun Liu,² Sheau-Shong Bor,³ Tian-Fu Hung,¹ and Chi Chiang Chen³

¹Ph.D. Program in Electrical and Communication Engineering, Feng Chia University, Tai-Chung, 40724, Taiwan, Republic of China

²Department of Electrical Engineering, Ching Yun University, Chung-Li, Tao-yuan, 32097, Taiwan, Republic of China; Corresponding author: jichyun@cyu.edu.tw

³Department of Electrical Engineering, Feng Chia University, Tai-Chung, 40724, Taiwan, Republic of China

Received 16 May 2012

ABSTRACT: This article presents a novel triband circular/elliptical polarized single-feed circular slot antenna for wireless local area network and worldwide interoperability for microwave access systems.